

# Robotic *in situ* stiffness cartography of InP membranes by dynamic force sensing

Jean-Ochin Abrahamians<sup>1,2</sup>, Bruno Sauvet<sup>1</sup>, Jérôme Polesel-Maris<sup>2</sup>, Rémy Braive<sup>3,4</sup> and Stéphane Régnier<sup>1</sup>

**Abstract**—Typical methods of measuring mechanical properties at the micro-scale are destructive, and do not allow proper characterisation on resonant MEMS/NEMS. In this paper, a cartography of local stiffness variations on a suspended micro-membrane is established for the first time, by a tuning-fork-based dynamic force sensor inside a SEM. Experiments are conducted on InP membranes 200nm thin, using a 9-DoF nanomanipulation system, complemented with virtual reality and automation tools. Results provide stiffness values ranging from 0.6 to 3 N/m on a single sample.

## I. INTRODUCTION

As of now, the behaviour of micro- and nano-scale resonators is not fully understood due to nonlinearities in their dynamics [1]. Research on the subject primarily consists in modelling and analysis. Reliable values from actual measurements of their mechanical properties are desired in order to provide the parameters to be used in simulations, confirm current suppositions concerning these small-scale dynamics, and predict their resonant behaviour. Typical measurement methods involve inherently destructive protocols which either rely on indenting samples, or applying enough pressure to deflect MEMS sensors. These methods can make the measurement itself unreliable [2]. Furthermore, they do not allow precise mapping of several points on a single sample, as the mechanical properties of the sample are potentially modified after each measurement.

Suspended micro-membranes (Fig. 1) are especially fragile (Fig. 2). Hence, non-destructive measurement on these samples first requires non-destructive mechanical positioning with accurate nanometer-range resolution. Since accurate manipulation has to be conducted by nanometric steps, it is excessively time-consuming if entirely handled by unassisted human operators. Automating some of the repetitive positioning operations is useful in alleviating the workload. This semi-automation brings the duration of experiments down to achievable levels for research purposes, and is an important first step before full automation. Virtual reality is another practical tool which, in addition to facilitating manual operations and providing a representation of confined

setups, can run simulations concurrent to the experiment. Developing these tools is part of the process towards enabling meticulous manipulation. Although the state of the art in micro-robotics now provides actuators which are accurate and dexterous enough to perform the required operations in terms of positioning and control, invasive measurement methods are unsuitable for use on micro-membranes. Therefore, the aim of this work is to demonstrate a proof of concept for a micro-scale stiffness cartography measurement method on fragile structures. Herein, the stiffness of a suspended InP membrane is locally measured by contact at several points of its surface, using a self-sensing quartz tuning fork probe controlled in frequency modulation. Experiments are conducted *in situ* through a robotic nanomanipulation system implemented in a scanning electron microscope. Section II summarises the state of the art in micro-robotics, and mechanical properties measuring, relevant to this study. Section III details the equipment and manipulation setup. Section IV describes the stiffness measurement method, and the experimental results thereby obtained.

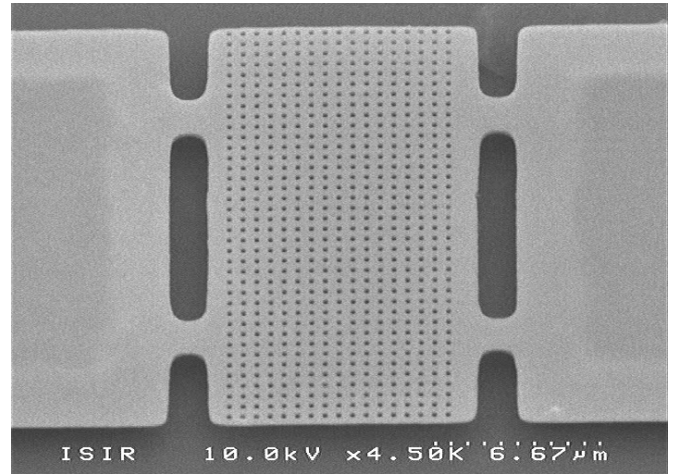


Fig. 1. Suspended membrane. Dimensions 10x20  $\mu\text{m}$ , thickness 200 nm.

## II. STATE OF THE ART

### A. Micro-robotic manipulation

Nowadays, micro-manipulation experiments are often performed under SEMs (scanning electron microscopes) rather than optical microscopes, partly because classical optical microscopy reaches its limits in resolution, but mainly because

<sup>1</sup> Institut des Systèmes Intelligents et de Robotique, Université Pierre et Marie Curie, CNRS UMR 7222, 4 Place Jussieu, 75005 Paris, France. {abrahamians, regnier}@isir.upmc.fr

<sup>2</sup> CEA, IRAMIS, Service de Physique et Chimie des Surfaces et Interfaces, F-91191 Gif-sur-Yvette, France.

<sup>3</sup> LPN-CNRS, Laboratoire de Photonique et de Nanostructures, 91460 Marcoussis, France

<sup>4</sup> Université Denis Diderot, 75205 Paris, France

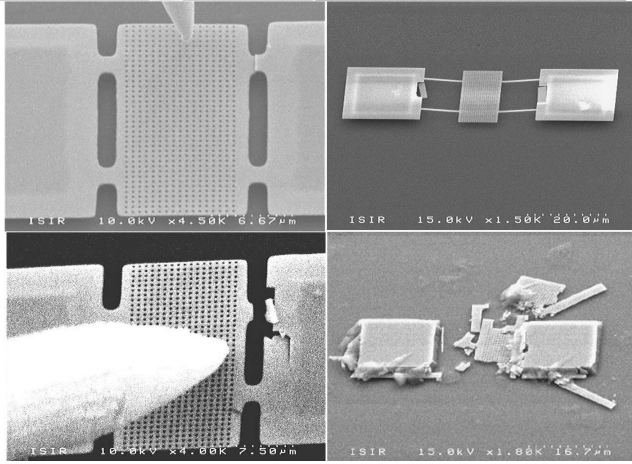


Fig. 2. Above: destroyed hinge (left) or destroyed suspension pads (right) due to electrostatically induced collisions between the tip of the probe and a sample. Below: consequences of careless manipulation of the local probe.

of the benefits of the significant depth and field of view offered by a SEM. This asset is most convenient at small scales, not only to bring the tools within operating range of the targeted samples, but also for the manipulation of any three-dimensional object. It is thus used for *in situ* electrical [3] or mechanical [4] characterisation, including mechanical characterisation of biological samples like cells [5]. In such experiments, the SEM can also be coupled with FIB (focused ion beam) [6] or STM (scanning tunneling microscope) [7] techniques. Challenges posed by the use of a typical SEM are largely related to the implementation of the experiment in the vacuum chamber and its operation under an electron beam. All materials must be vacuum-compatible to prevent outgassing. Specific measures must also be taken towards heat dissipation from the equipment, as there is no convection cooling. Furthermore, tools and samples must be conductive enough to prevent electrostatic charging. Current-generation SEMs and ESEMs can allow for more leeway regarding these requirements. As for the micro-manipulation platforms, commercially available actuators offer nanometer-scale resolution over up to millimeter-scale travel ranges. Sub-nanometer resolution can comparatively be achieved over micrometer-scale travel ranges, and the desired degrees of freedom (DoF) are obtained by assembling axial positioners. Delicate micro-manipulation also greatly benefits from being complemented by virtual reality and haptics [8]. Such techniques have for instance been employed inside a SEM for the micro-manipulation of organs, capillaries and cells [9], by coupling probes and manipulation tools with a commercial haptic device. Technical performances in virtual imaging are more common in AFM (Atomic Force Microscopy) but had not yet been exploited for the mapping of mechanical properties. Coupling a manipulation system with virtual reality and automated control helps in achieving these measurements on fragile structures.

## B. Mechanical properties of membranes

Micro-scale membranes are often fragile due to their thinness and suspended architecture. Interest lies in characterising resonators in their operating configuration, therefore the measurement method must not induce any displacement prone to affect the suspension or rupture the hinges. Further, a cartography requires measurements on several points without compromising the sample. The main methods of mechanical characterisation at the micro-scale are MEMS-based and classical AFM-based techniques. MEMS-based techniques rely on buffering beam deflection [10] or indentation [5]. Classical AFM-based techniques mainly involve the deflection of a cantilever and are equally destructive, but can be complemented by CNTs to offer greatly increased sensitivity. [11] Mechanical characteristics can be obtained through models [12], though they require measurements in the first place. At a larger scale, vibrational techniques have been used for the local mechanical characterisation of thin films [13]. The approach proposed here is a micro-scale vibrational method which does not involve any strain or deflection, using a resonator-based dynamic force sensor as a local probe.

## C. Tuning forks as sensors

Tuning forks have been mainly used in AFM in the qPlus configuration [14]. In that configuration, a probe tip is attached to one prong, and the other is fixed. The high sensitivity and stiffness of these sensors have been exploited in developing non-destructive imaging, including non-contact imaging. They have been admirably used for sub-atomic resolution AFM [15]. Self-sensing resonator AFM techniques are not limited to quartz tuning forks and can be applied with other models, including monolithic crystal resonators. Commercially available resonators exist in various geometries and eigenfrequencies, which can be used for higher imaging speed and increased dexterity in manipulation [16]. Besides the non-destructive aspect, there are practical advantages to using these self-sensing probes instead of the classical microfabricated cantilevers, not the least of which is the relative simplicity of implementation under an electron beam. The sensor used in this work doesn't have a fixed prong, and benefits from the high sensitivity and small oscillation amplitude of the tuning fork for non-destructive operations. Although its principle is identical to that of an AFM, it is used for mechanical characterisation rather than microscopy.

## III. MANIPULATION SETUP

### A. Overview of the robotic manipulation system

The nanorobotic manipulation system (Fig. 3) is implemented in a Scanning Electron Microscope (Hitachi S-4500). It consists in a 3-DoF Cartesian manipulator and a 6-DoF "hexapod" sample holder platform (SmarAct GmbH, custom-built). Both are composed of closed-loop axial stick-slip actuators. The hexapod's mobility is used to obtain the desired angle between the tool and the sample through its 3 rotational DoF. The actuators offer an ascertained resolution better than 2 nm over a travel range of 12 mm, and are

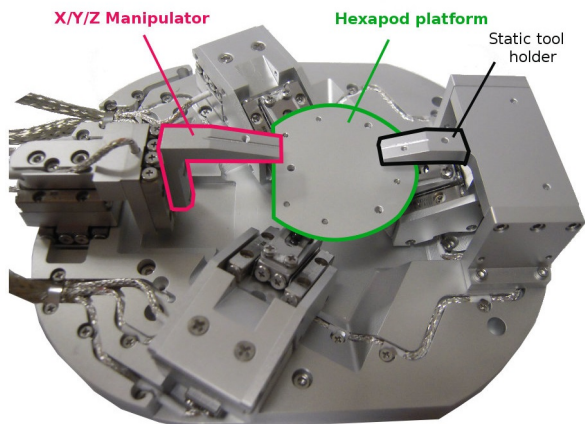


Fig. 3. Robotic manipulation platform (SmarAct GmbH); overall dimensions: 11x13x4 cm.

used both for coarse and fine positioning. Their closed-loop resolution is determined by the performance of their optical sensors [17]. The SEM view is used to calibrate the initial positioning of the tool relative to the samples, and identify the membrane amongst a batch to operate on *in situ*. The large travel range of the actuators is taken advantage of to access any membrane from a large batch. The whole platform can be tilted at an angle up to 45° to discern and accurately control the point where the tip of the probe touches the sample.

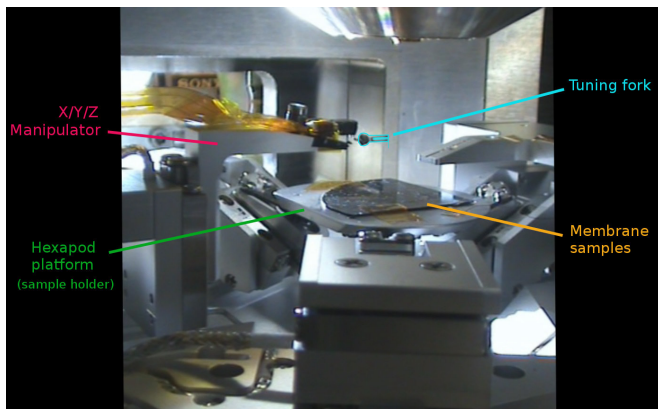


Fig. 4. Manipulation setup inside the SEM vacuum chamber.

### B. Probe fabrication and integration

The probe used in this paper was fabricated using a CF308 quartz tuning fork (Citizen America) removed from its canister, with a free resonance frequency of 32.768kHz. The probe is composed of the tuning fork, with a tungsten probe tip of 1-2 mm length with a tip radius <100 nm (T-4-5 Picoprobe, GGB Industries) manually glued on the side of one prong using conductive silver epoxy (EPO-TEK H21D, Epoxy Technology). The resulting unbalance reduces the quality factor of the tuning fork, so the weight is then compensated by adding a small deposit of epoxy on the other prong (Fig. 5). The tip is connected to ground through the electrode of the prong it is attached to, to prevent its

electrostatic charging under the electron beam. Its use as a local stiffness sensor is explained in Section IV. The tuning fork is then fixed on the manipulator. The probe is connected to a custom electronic preamplifier adapted for use under the electron beam of the microscope [18], and an oscillation control system (OC4-Station, SPECS-Nanonis) with a data acquisition card as previously described in [19].

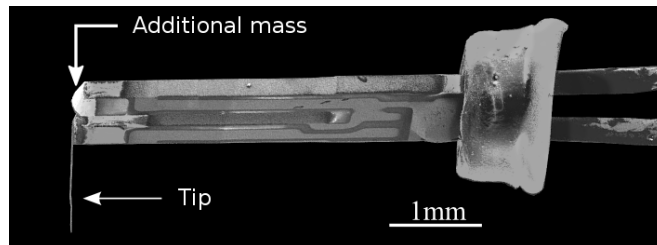


Fig. 5. 35° inclined top view of the tuning fork probe by SEM. During a measurement, the apex of the tip is brought into contact with the samples.

### C. Virtual Reality interface

Both the hexapod and the manipulator can be driven manually from a control unit, or by remote control through their virtual counterparts on a computer (Fig. 6). This virtual reality system includes a 3D model of the manipulation unit, rendered in the physics engine of the Blender software (open-source, Blender Foundation). While it does allow unskilled operators to interact with the nano-world, it is mainly designed as a practical tool to assist experienced manipulators by providing a free view of the operation, which can be rotated around or magnified on the area of interest. Once calibrated, the virtual reality system allows the user to swiftly and safely bring the tool within operating range, close to the sample. The view offered by a SEM can be insufficient due to its being two-dimensional, and might even be macroscopically cluttered or otherwise obstructed during experiments. The real-time 3D visualisation thus completes the qualitative SEM view with quantified distances. Virtual reality can also provide a representation of a geometrically known sample as a visual reference, in order to operate without continuous use of the microscope view. This can be useful for samples that risk deteriorating if exposed to the SEM electron beam for extended periods of time, but also to pre-visualise nanohandling sequences. This can also be extended to the use of equipment which cannot function simultaneously with the electron beam.

## IV. STIFFNESS MEASUREMENTS

### A. Principle of tuning fork stiffness measurement

In a quartz tuning fork, the quartz crystal prongs oscillate when excited by the electrodes set on each prong. The oscillation amplitude is of a few Ångströms or less. Due to the design of the electrodes, the tuning fork is excited in its anti-phase coupled oscillation mode. All mentions of resonance henceforth refer to this mode.

Dynamic force sensing with a tuning fork can be done in AM/PM (Amplitude/Phase Modulation) or FM (Frequency

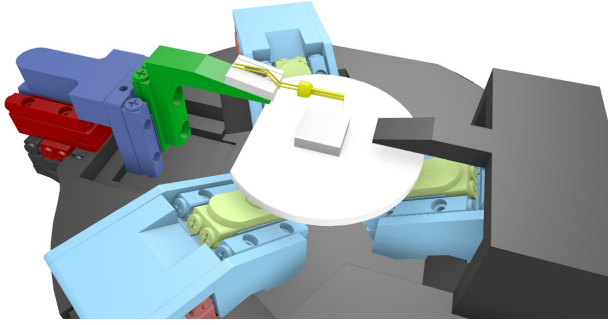


Fig. 6. Blender virtual reality system interface.

Modulation) modes. Here, the tuning fork is used in FM mode to benefit from its high quality factor. [19] The quality factor  $Q$  is related to the tuning fork's sensitivity.  $Q$  is considerably higher in a vacuum, as there is no energy loss from friction with air molecules. In a  $10^{-4}$  Pa vacuum, the manufactured sensors have  $Q$  ranging from 20000 to 60000 (versus 5000 to 10000 in the air). The sensor used in this paper has a  $Q$  of 30000, including the tip.

In FM mode, an electrical excitator applies a voltage to the tuning fork to drive it at its resonance frequency  $f_0$ , and feeds back the resulting current in a preamplifier for regulation by the PLL (phase-locked loop) and an AGC (automatic gain control), analysing its frequency shift while keeping constant both phase and amplitude. The relation between frequency shift  $\Delta f$  and sample stiffness  $k_{sample}$  is obtained using the coupled oscillators model presented in [20] (Fig. 7), which unlike single-cantilever models, takes into account oscillation dynamics as affected by the coupling of the two prongs of the tuning fork - with each prong a harmonic oscillator modelled as a clamped beam.  $\Delta K$  represents the effective stiffness of the combined tip and sample,

$$\Delta K = \frac{1}{\frac{1}{k_{tip}} + \frac{1}{k_{sample}}} \quad (1)$$

It is assumed that the tip is much stiffer than the sample, and therefore  $k_{sample} \approx \Delta K$ . The resolution of this model gives  $k_{sample}$  proportional to  $\Delta f$  factored by the tuning fork sensor sensitivity

$$k_{sample} = \left( \frac{2k_{probe}}{f_0} \right) \Delta f \quad (2)$$

with  $k_{probe}$  the effective elastic constant of the whole tuning fork probe, including the added probe tip and its counterweight. There are several ways to measure  $k_{probe}$ . [21] The value used in this paper is  $10.7 \times 10^3$  N/m [22] and relies on a geometrical method, which sums up the stiffness of both prongs based on their dimensions and materials, and evaluates the coupling elastic constant at 20-35% of the total. [20]

### B. Manipulation protocol

The experiments aim to successively measure the stiffness on several points along the surface of a suspended micro-

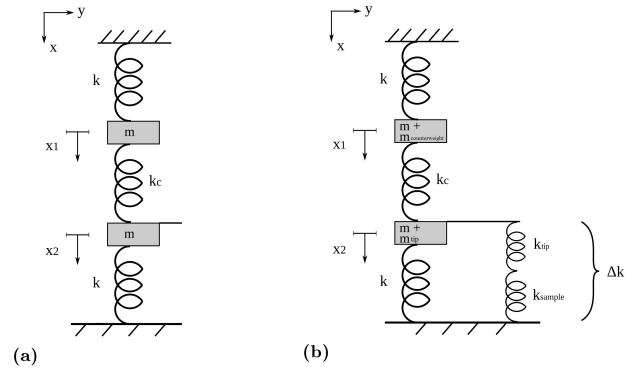


Fig. 7. Spring-mass mechanical models of (a): a free tuning fork [20], and (b): a tuning fork with a probe tip in contact with a sample. Both prongs have the same mass  $m$  and stiffness  $k$ ;  $k_c$  models the coupling between the prongs; the tip and the counterweight have the same mass  $m_{probe}$ .

membrane. They are carried out through the following steps:

1) *Coarse approach*: The tool is initially brought down to 50  $\mu\text{m}$  above the samples, instantly by using the virtual reality controls after the system is calibrated, or manually using the microscope vision's rough depth-from-focus otherwise. The origin distance calibration is done by contact between the probe and a sample, and is renewed every time a new probe is set on the manipulator, or a new sample is set on the hexapod.

2) *Fine approach*: The final part of the approach is conducted automatically by nanometric steps, using the frequency shift feedback from the sensor. Because of the pull-in interaction forces between the probe tip and the substrate (Fig. 8), the detection is triggered without any contact, and as far as 100 nm above the sample.

3) *Angle adjustment*: The angle of incidence of the tip can be adjusted by probing the depth coordinates of three points around the area of interest on the membrane, determining the inclination of the associated plane in the tool's frame of reference, then compensating it with the hexapod. The verticality of the tip relative to the sample is thus ensured, which enables the use of the simplified theoretical model (Fig. 7) which assumes there are no shearing forces. This is especially useful as compressed InP membranes can take various topographical shapes, bending either inwards or outwards, and a single membrane can thereby have its inclination varying across its surface. (Fig. 9)

4) *Measurement*: The measuring process is automated from a computer tapping into the data from the manipulator and sensor systems. The contact between the apex of the tip and the sample is denoted by an increasing value of the frequency shift, and second order-response oscillating variations of the oscillation amplitude which can be observed when the controller starts compensating for the contact with the membrane. (Fig. 10) A stable frequency shift value is reached after a few seconds. Pushing the probe further down most often results in the membrane or its hinges breaking in a visually obvious way. Even if the sample seems to remain intact, such invalid measurements are easily discarded: either



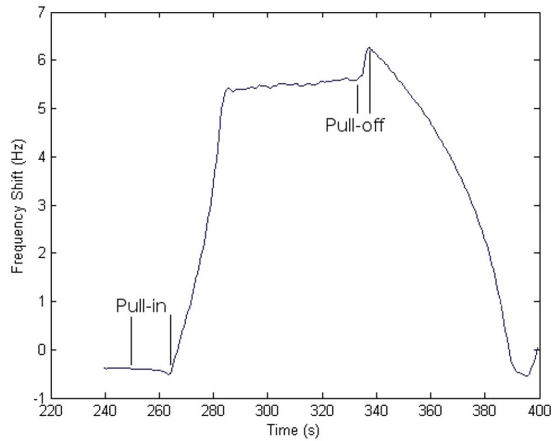


Fig. 8. Frequency shift during a slow measurement operation. The electrostatic and van der Waals interaction forces are displayed before reaching the sample: the frequency shifts up to a few mHz between 150nm and 50nm above the sample (electrostatic pull-in), and up to a few dozen mHz below 50nm (van der Waals pull-in). After taking a measurement, if the probe is withdrawn back up by nanometric steps rather than suddenly, a pull-off resistance resulting from adhesion forces can be observed.

the obtained frequency shift value is unstable, or the probe tip first gets noticeably deflected onto the surface, presumably due to the membrane being stuck to the substrate. This deflection can be observed using the SEM view. Frequency shift values can also be positive yet unstable in the non-contact zone, very close to the sample. In this case, lowering the probe by one nanometer leads to true contact and a stable value. The true measurement point is therefore always defined as the single stable value obtained after the tip enters into contact with the membrane, without being deflected, and while the sample is neither deformed nor indented.

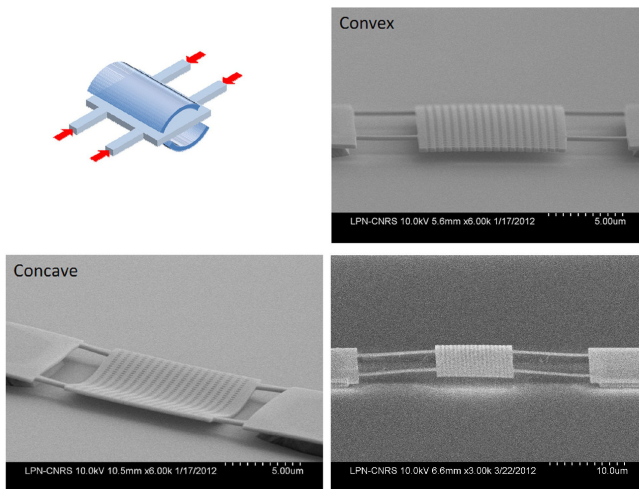


Fig. 9. InP membranes are stretched or compressed by 20 nm during fabrication. Compressed membranes can bend in either direction, the exact resulting shape depending on the geometry and position of the hinges.

### C. Results

Cartography experiments were conducted on suspended InP membranes 200nm thin. (Fig. 1) Their fabrication was



Fig. 10. Shape of the frequency shift (upper curve) and amplitude (lower curve), spanning 1 second, upon entering into contact with a surface (Nanonis software). Frequency shifts data starts increasing towards its value measured by the pre-amplifier. Amplitude oscillates from a second order response as it is regulated by the PLL and AGC.

first described in [23]. The InP membranes are grown by epitaxy and structured by wet etching. Their shape is rectangular with dimensions  $10 \times 20 \mu\text{m}$ , and they are patterned with air-holes of diameter less than 200 nm. Each membrane is suspended between two supporting pads and held by four hinges. Local stiffness measurements show values varying greatly along the surface of the membrane. The highest stiffness values are obtained on the hinges, and two- to five times lower values can be obtained near the center of the membrane depending on its compression type. Fig. 11 shows local stiffness measurements between two hinges of a concave membrane ranging from 0,6 to 3 N/m. The oscillation amplitude of the tuning fork is non-destructive, and estimated around 700 pm using a method described in [24]. Repeated measurements on the same point were found to fall within 5 % of the same value, on a sample size of a dozen. This repeatability demonstrates that the measurement method is indeed non-destructive. While the InP membranes are themselves semi-conductive, the samples were fabricated on a non-conductive  $\text{SiO}_2$  substrate and were studied *in situ*, which accounts for the strong potentially destructive electrostatic effects encountered during the experiments.

### V. CONCLUSION

A non-destructive local stiffness measurement method has been implemented, based on the works on tuning fork AFM. A 9-DoF platform has been used for nano-manipulation, assisted by virtual reality and automation tools for practical purposes. Over twenty measurements were taken *in situ* amongst a manufactured batch on a single membrane without altering the sample. Such measurements are to provide parameters for the simulations on which current studies rely for analysis. This will contribute to the understanding of the mechanical properties of micro-membrane resonators, through the relations between their geometries, their stiff-

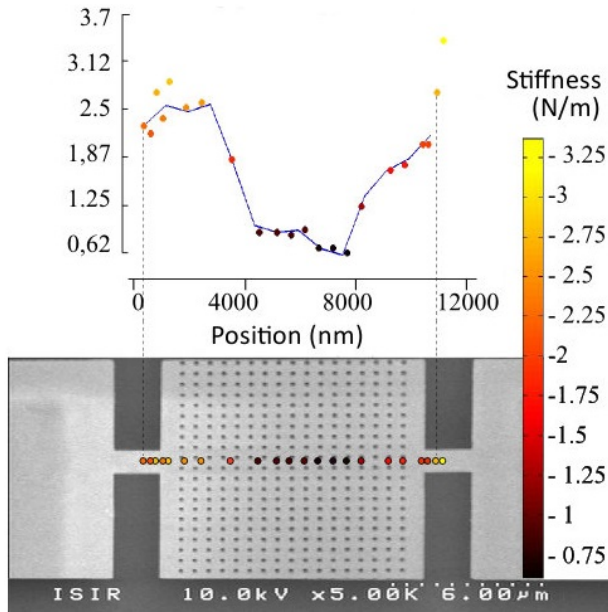


Fig. 11. Stiffness measurements ranging between two suspensions of a membrane, taken from left to right. The sample is left undamaged.

ness and the local distributions thereof, as well as the eigenmodes of their structures. Ensuing knowledge of the nonlinearities in their mechanical behaviour will be further relevant to the understanding of their quantum dynamics [25]. The chosen approach to measuring the stiffness of resonant MEMS/NEMS is validated. Further applications of this concept can be derived on even thinner samples. However, proper characterisation of actuators will be required, along with positioning resolutions in the sub-nanometer range, to fully benefit from the low oscillation amplitudes of the probes.

## VI. ACKNOWLEDGMENT

This work was supported by the French Agence Nationale de la Recherche, through the NANOROBUST project (contract ANR 2011 NANO 006).

## REFERENCES

- [1] J. F. Rhoads, S. W. Shaw, and K. L. Turner, "Nonlinear dynamics and its applications in micro- and nanoresonators," *Journal of Dynamic Systems, Measurement, and Control*, vol. 132, no. 3, p. 034001, 2010.
- [2] L. Qiao and X. Zheng, "Effect of surface stress on the stiffness of micro/nanocantilevers: Nanowire elastic modulus measured by nanoscale tensile and vibrational techniques," *Journal of Applied Physics*, vol. 113, no. 1, pp. 013 508–013 508–9, Jan. 2013.
- [3] M. Elawayeb, Y. Peng, K. J. Briston, and B. J. Inkson, "Electrical properties of individual NiFe/Pt multilayer nanowires measured in situ in a scanning electron microscope," *Journal of Applied Physics*, vol. 111, no. 3, pp. 034 306–034 306–4, Feb. 2012.
- [4] X. Ye, Y. Zhang, and Y. Sun, "Robotic pick-place of nanowires for electromechanical characterization," in *IEEE International Conference on Robotics and Automation*, May 2012, pp. 2755–2760.
- [5] Y. Shen, M. Nakajima, M. Homma, and T. Fukuda, "Auto nanomanipulation system for single cell mechanical property characterization inside an environmental SEM," in *IEEE/RSJ International Conference on Intelligent Robots and Systems (IROS)*, Oct. 2012, pp. 646–651.
- [6] V. Eichhorn, M. Bartenwerfer, and S. Fatikow, "Nanorobotic assembly and focused ion beam processing of nanotube-enhanced AFM probes," *IEEE Transactions on Automation Science and Engineering*, vol. 9, no. 4, pp. 679–686, Oct. 2012.
- [7] S. Qin, T.-H. Kim, Z. Wang, and A.-P. Li, "Nanomanipulation and nanofabrication with multi-probe scanning tunneling microscope: From individual atoms to nanowires," *Review of Scientific Instruments*, vol. 83, no. 6, pp. 063 704–063 704–4, Jun. 2012.
- [8] A. Bolopion, H. Xie, D. Haliyo, and S. Régnier, "Haptic teleoperation for 3-d microassembly of spherical objects," *IEEE/ASME Transactions on Mechatronics*, vol. 17, no. 1, pp. 116–127, 2012.
- [9] M. Takahashi, H. Ko, T. Ushiki, and F. Iwata, "Interactive nano manipulator based on an atomic force microscope for scanning electron microscopy," in *International Symposium on Micro-NanoMechatronics and Human Science (MHS)*, Nov. 2011, pp. 495–500.
- [10] Y. Shen, M. Nakajima, Z. Yang, M. Homma, and T. Fukuda, "Nano needle with buffering beam for single cell stiffness measurement by nanorobotic manipulators inside ESEM," in *IEEE Conference on Nanotechnology*, Aug. 2012, pp. 1–4.
- [11] F. Arai, M. Nakajima, L. Dong, and T. Fukuda, "Pico-newton order force measurement using a calibrated carbon nanotube probe by electromechanical resonance," in *IEEE International Conference on Robotics and Automation*, 2003, pp. 300–305.
- [12] P.-H. Chen, C.-H. Yang, C.-Y. Tsai, T.-L. Chang, W.-C. Hsu, and T.-C. Chen, "Young's modulus of high aspect ratio Si<sub>3</sub>N<sub>4</sub> nano-thickness membrane," in *IEEE Conference on Nanotechnology*, Aug. 2007, pp. 1341–1344.
- [13] D. Goto, T. Namazu, S. Inoue, T. Takeuchi, K. Murakami, E. Komatsu, Y. Kawashimo, and T. Takano, "Young's modulus measurement method for nano-scale film materials by using MEMS resonator array," in *Solid-State Sensors, Actuators and Microsystems*, Jun. 2009, pp. 1321–1324.
- [14] F. J. Giessibl, "High-speed force sensor for force microscopy and profilometry utilizing a quartz tuning fork," *Applied Physics Letters*, vol. 73, no. 26, pp. 3956–3958, Dec. 1998.
- [15] F. J. Giessibl, S. Hembacher, H. Bielefeldt, and J. Mannhart, "Subatomic features on the silicon (111)-(77) surface observed by atomic force microscopy," *Science*, vol. 289, no. 5478, pp. 422–425, Jul. 2000.
- [16] J. C. Acosta, J. Polesel-Maris, F. Thoyer, H. Xie, S. Haliyo, and S. Régnier, "Gentle and fast atomic force microscopy with a piezoelectric scanning probe for nanorobotics applications," *Nanotechnology*, vol. 24, no. 6, p. 065502, Feb. 2013.
- [17] Y. L. Zhang, Y. Zhang, C. Ru, B. Chen, and Y. Sun, "A load-lock-compatible nanomanipulation system for scanning electron microscope," *IEEE/ASME Transactions on Mechatronics*, vol. 18, no. 1, pp. 230–237, Feb. 2013.
- [18] J. Polesel-Maris, "Electronic control and amplification device for a local piezoelectric force measurement probe under a particle beam," WO Patent 2011/092 225 A1, Aug., 2011.
- [19] J. C. Acosta, G. Hwang, J. Polesel-Maris, and S. Régnier, "A tuning fork based wide range mechanical characterization tool with nanorobotic manipulators inside a scanning electron microscope," *Review of Scientific Instruments*, vol. 82, no. 3, pp. 035 116–035 116–8, Mar. 2011.
- [20] A. Castellanos-Gomez, N. Agrait, and G. Rubio-Bollinger, "Dynamics of quartz tuning fork force sensors used in scanning probe microscopy," *Nanotechnology*, vol. 20, p. 215502, Mar. 2010.
- [21] H. Xie, J. Vitard, S. Haliyo, S. Régnier, and M. Boukallel, "Calibration of lateral force measurements in atomic force microscopy with a piezoresistive force sensor," *Review of Scientific Instruments*, vol. 79, no. 3, pp. 033 708–033 708–6, Mar. 2008.
- [22] B. Sauvet, "Design of a microrobotic platform for the manipulation and characterization of thin films," Ph.D. dissertation, Université Pierre et Marie Curie, Paris, Mar. 2013.
- [23] M. Strassner, J.-L. Leclercq, and I. Sagnes, "Fabrication of ultra-thin InP membranes and their application for high reflective mirrors in tunable vertical-cavity devices," in *International Conference on Indium Phosphide and Related Materials (IPRM)*, Jun. 2004, pp. 221–223.
- [24] A. Makky, T. Berthelot, C. Feraudet-Tarisse, H. Volland, P. Viel, and J. Polesel-Maris, "Substructures high resolution imaging of individual IgG and IgM antibodies with piezoelectric tuning fork atomic force microscopy," *Sensors and Actuators B: Chemical*, vol. 162, no. 1, pp. 269–277, Feb. 2012.
- [25] T. Antoni, K. Makles, R. Braive, T. Briant, P.-F. Cohadon, I. Sagnes, I. Robert-Philip, and A. Heidmann, "Nonlinear mechanics with suspended nanomembranes," *Europhysics Letters*, vol. 100, no. 6, p. 68005, Dec. 2012.